Type-II CdS nanoparticle–ZnO nanowire heterostructure arrays fabricated by a solution process: enhanced photocatalytic activity†

Youngjo Tak, Hyeyoung Kim, Dongwook Lee and Kijung Yong*

Received (in Cambridge, UK) 18th June 2008, Accepted 4th August 2008
First published as an Advance Article on the web 27th August 2008
DOI: 10.1039/b810388g

We report a two-step, solution-based synthetic method to fabricate CdS nanoparticles-sensitized ZnO nanowire heterostructure arrays which showed enhanced photocatalytic activities in comparison with bare ZnO nanowire arrays.

Numerous research efforts have been concentrated on the environmental use of semiconductor photocatalysts in processes such as the decomposition of toxic organic compounds and hydrogen production *via* water splitting.[1] Among the various photocatalytic semiconductor materials, metal-oxide semiconductors such as ZnO (3.2 eV), TiO_2 (3.2 eV), α-Fe_2O_3 (3.1 eV) and WO_3 (2.8 eV) have been researched intensively as practically applicable photocatalysts because they show high photocatalytic activities and synthetic routes to them are economical.[2] However, these single metal-oxide photocatalysts have wide band-gap energies, which are disadvantageous to absorption and use of the visible light region of solar energy. To improve photocatalytic activities, composite semiconductor photocatalyst systems have received a great deal of attention because of two important reasons. First, in the composite semiconductor systems with different energy levels, wide band-gap semiconductors can utilize visible light by coupling narrow band-gap semiconductor photosensitizers.[3] Second, charge injection from one semiconductor into another can lead to efficient and longer charge separation by reducing the electron–hole pair recombinations.[4]

Various types of ZnO micro/nanomaterials have been studied for photocatalyst applications.[5] However, there are difficulties in collecting and recycling powder-type photocatalysts after use. Recently, 1-D ZnO nanostructure arrays, such as nanowires[6] and nanobelts,[7] have been tested as immobilized photocatalysts due to their expected high photocatalytic activity resulting from large surface-to-volume ratio, and recyclable characteristics. However, there are few reports of composite ZnO nanowire arrays to enhance the photocatalytic efficiency. In this communication, we report a facile two-step solution-based method to fabricate a novel CdS nanoparticle (NP)/ZnO nanowire (NW) heterostructure array. This interesting heterostructure array showed enhancement of the visible light absorption and also photocatalytic activity due to efficient charge separation by their type-II band alignments.

Surface Chemistry Laboratory of Electronic Materials, Department of Chemical Engineering, Pohang University of Science and Technology (POSTECH), Pohang 790-784, Korea. E-mail: kyong@postech.ac.kr; Fax: +82-54-279-8298; Tel: +82-54-279-2278

† Electronic supplementary information (ESI) available: AM 1.5G spectrum. See DOI: 10.1039/b810388g

We grew ZnO nanowire arrays on silicon substrates using the ammonia solution hydrothermal method reported elsewhere.[8] Prepared samples were post-annealed in air ambient at 400 °C for 1 h to enhance the crystallinity and chemical stability for the following CdS chemical bath deposition (CBD) process. For the nucleation and growth of CdS nanoparticles on the ZnO nanowire surface, the ZnO nanowire array substrate was immersed in an aqueous solution containing $CdSO_4$: thiourea : NH_4OH = 1 mM : 50 mM : 0.5 M at the solution temperature of 60 °C. The reaction time was 100–200 min.

To examine the photocatalytic activity, orange-II (4-(2-hydroxy-1-naphthylazo)benzenesulfonic acid, Aldrich) dye was chosen for the photodecomposition study. Bare ZnO NW, as-prepared CdS NP/ZnO NW and post-annealed CdS NP/ZnO NW array samples, cut into the same size of 1 cm × 2 cm, were horizontally immersed in 2–2.5 mL of 1.0×10^{-5} M orange-II solution and irradiated by a UV-lamp (15 W centered at 365 nm, 2 mW cm^{-2}, Uvitec-LF215LM). The remaining amounts of dye in the solution were determined by measuring the absorption intensity at 486 nm, a main peak position of the orange-II dye, using a UV2501PC (SHIMADZU) spectrometer.

Fig. 1(a) is a schematic diagram showing the fabrication process of the CdS NP/ZnO NW heterostructure array, and Fig. 1(b) and (c) show the morphology of the bare ZnO nanowire and the CdS NP/ZnO NW heterostructure array, respectively, observed by field-emission scanning electron microscopy (FE-SEM). Bare ZnO nanowires were grown

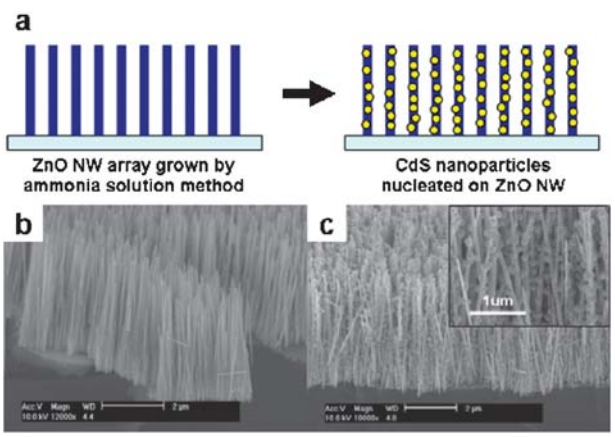

Fig. 1 (a) Schematic diagram of the two-step solution process to fabricate a CdS NP/ZnO NW heterostructure array. FE-SEM images of (b) bare ZnO NW and (c) CdS NPs coated ZnO NW array.

vertically on a large area of the substrate with a diameter of 50–100 nm and a length of 4–5 μm. After the CBD process, we could observe that CdS nanoparticles, which have diameters in the range 50–100 nm, uniformly nucleated on the ZnO nanowire surfaces from the tip to the bottom.

The detailed microscopic structure and chemical composition of the CdS NP/ZnO NW heterostructure were analyzed using a high-resolution scanning transmission electron microscope (HR-STEM). Fig. 2(a) and (b) are low-magnification bright field (BF) and high angle annular dark field (HAADF) images of the sample. They show uniformly attached CdS nanoparticles with bright contrast on the ZnO nanowires. A high-resolution image of the CdS/ZnO heterojunction region (Fig. 2(c)) and corresponding fast Fourier transform (FFT) (Fig. 2(d)) reveal that polycrystalline CdS nanoparticles were grown on a single crystalline ZnO nanowire and both materials have hexagonal crystal phases with atomic plane spacings corresponding to the JCPDS No. 79-2205 (ZnO) and 80-0006 (CdS). Fig. 2(e) is a scanning TEM (STEM) image of a CdS NP/ZnO NW heterostructure and (f–i) show corresponding EDX elemental mapping of Zn, O, Cd and S, respectively. It is noticeable that Cd and S elements are localized at the nanoparticle region in the image.

The crystallinity and optical absorption properties of the CdS NP/ZnO NW heterostructure array depending on the annealing treatments were investigated by XRD and UV–visible spectroscopy. Fig. 3(a) shows digital camera images of the bare ZnO NW, as-prepared CdS NP/ZnO NW and post-annealed CdS NP/ZnO NW samples. From the XRD data (Fig. 3(b)), we could observe that both as-prepared and 400 °C Ar-annealed samples had a hexagonal ZnO(002) peak

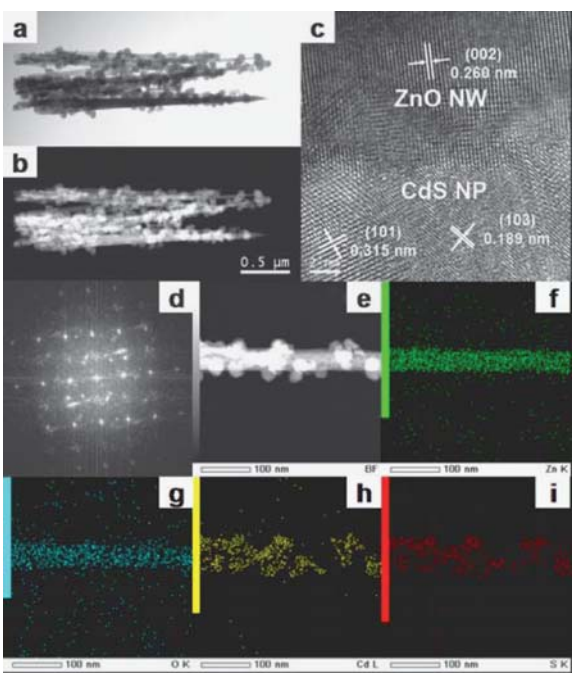

Fig. 2 (a) Bright field (BF) and (b) high angle annular dark field (HAADF) STEM images of CdS NP/ZnO NW heterostructures. (c) High-resolution TEM image of the CdS/ZnO heterojunction region and (d) corresponding FFT. (e) STEM image and corresponding EDX elemental mapping of (f) Zn, (g) O, (h) Cd and (i) S, respectively.

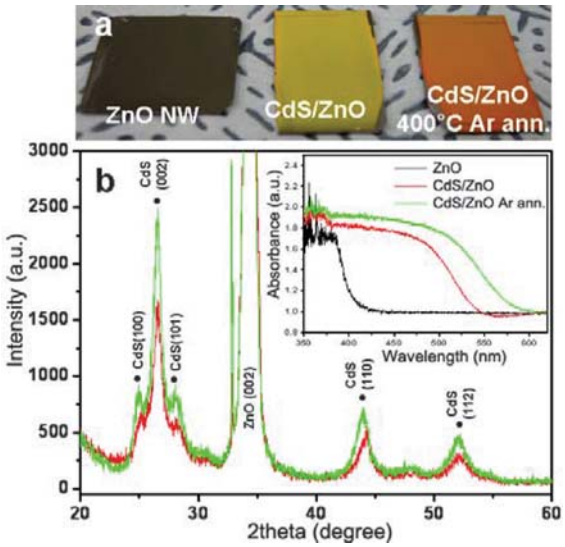

Fig. 3 (a) Digital camera image of the samples. (b) XRD data of the as-prepared and annealed CdS NP/ZnO NW. The inset shows diffused reflectance spectra (DRS) of the ZnO NW, as-prepared CdS NP/ZnO NW and post-annealed CdS/ZnO NW heterostructure arrays.

and CdS(100), (002), (101), (110), (112) peaks. These XRD peak positions are consistent with the atomic plane spacings in the HR-TEM image.

The intensities of the CdS related peaks increased slightly after the 400 °C Ar-annealing process. In contrast to the bare ZnO NW sample, CdS sensitized ZnO NW samples could absorb visible light and the absorption range increased up to ~580 nm after the annealing process (inset of Fig. 3(b)).

The photocatalytic activity of the CdS NP/ZnO NW heterostructures was evaluated by the degradation of an orange-II organic dye and compared with the bare ZnO NW.

Fig. 4 is a plot of the remaining dye concentration percentage of the initial dye concentration (C_o: 1.0×10^{-5} M) *versus* the UV irradiation time. Without any catalyst, it showed a slight increase in the orange-II concentration due to the slow evaporation of the solvent during the irradiation. This confirms the photostability of the organic dye. The CdS NP/ZnO NW heterostructure samples, both as-prepared and

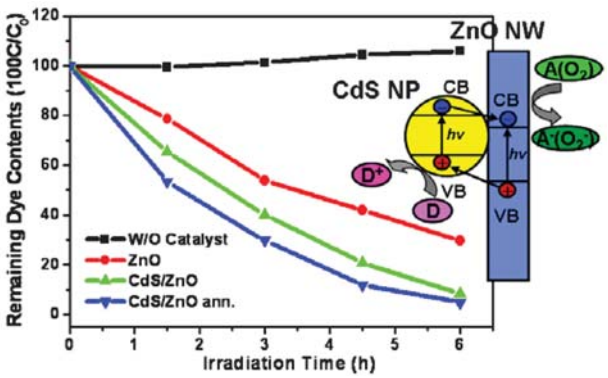

Fig. 4 Time dependent dye contents remaining in the solution after UV irradiation and schematic diagram showing the energy band structure and electron–hole pair separation in the CdS NP/ZnO NW heterostructure.

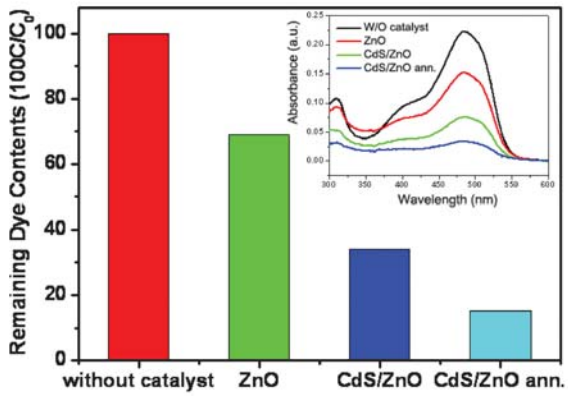

Fig. 5 Dye contents remaining in the solutions after 2 h solar-simulated light irradiation. Inset: absorption spectra of the photo-degraded dye solutions.

post-annealed ones, showed enhanced photocatalytic activities in comparison with the bare ZnO NW sample.

Possible reasons for the enhancement of the photocatalytic activity of the heterostructure photocatalysts are the increase in the specific photocatalyst area of the heterostructure and the coupling effects of ZnO NWs and CdS NPs. As shown in the schematic diagram, the band position of CdS and ZnO has a type-II structure. This type-II band alignment can efficiently separate electron–hole pairs which are photo-generated in each semiconductor material (*i.e.* ZnO and CdS) and reduce their recombination.[9] The photo-generated electrons transfer to the conduction band of ZnO NW and reduce the molecular oxygen O_2 to the superoxide radical anion $O_2^{\bullet -}$, producing hydroxyl radical $OH^{\bullet}$, which is a strong oxidizing agent to decompose the organic dye. The proposed mechanism for the photocatalytic decomposition of organic dye by CdS NP/ZnO NW heterostructures can be described as follows:[10]

$$CdS/ZnO + h\nu \rightarrow CdS(h^+)/ZnO(e^-)$$

$$ZnO(e^-) + O_2 \rightarrow O_2^{\bullet -}$$

$$O_2^{\bullet -} + H_2O \rightarrow HO_2^{\bullet} + OH^-$$

$$HO_2^{\bullet} + H_2O \rightarrow H_2O_2 + OH^{\bullet}$$

$$H_2O_2 \rightarrow 2OH^{\bullet}$$

$$OH^{\bullet} + \text{organic dye (orange-II)} \rightarrow CO_2 + H_2O$$

To demonstrate the effects of the visible light absorption ability of the heterostructures on the photocatalytic activity, we tested dye decomposition rates of the samples under conditions similar to natural solar-light irradiation. The natural solar-light was generated by a solar-simulator (300 W xenon arc lamp with AM 1.5G filter, 100 mW cm^{-2}, Oriel-91160). The inset of Fig. 5 shows absorption spectra of organic dye solution photo-degraded by bare ZnO NW, as-prepared CdS NP/ZnO NW and post-annealed CdS NP/ZnO NW samples after 2 h of solar-simulated light irradiation. It shows that 85% and 66% of organic dye was degraded by post-annealed CdS NP/ZnO NW and as-prepared CdS NP/ZnO NW arrays, respectively. In contrast, bare ZnO NW sample degraded only 31% of organic dye (Fig. 5). This result may originate from solar light absorption efficiency. As shown in the inset of Fig. 3, the bare ZnO nanowire array absorbs only in the UV region (300–400 nm) of the AM 1.5G spectrum which is a minor portion of the full spectrum intensity. However, the CdS/ZnO heterostructure array can absorb in the maximum intensity region (around 500 nm). Comparing the results for as-prepared CdS/ZnO and post-annealed CdS/ZnO samples, which have similar specific area, we suggest that the higher photocatalytic activities of the post-annealed CdS NP/ZnO NW sample in comparison with the as-prepared one result from increased visible light absorption and charge injection efficiency due to enhanced crystallinity as verified by XRD and DRS data (Fig. 3).

Another important point is that we did not use any sacrificial agents (hole-scavengers), such as alcohols or sulfide/sulfite ions, in the current study. Generally, the addition of hole-scavengers is known to remarkably increase the photocatalytic efficiency and the photo-corrosion stability of sulfide catalysts.[11] Therefore, there is plenty of scope for improvement of the photocatalytic properties of our heterostructures in future studies.

In summary, we prepared CdS NP/ZnO NW heterostructure arrays using a facile two-step solution method. It was found that the CdS NP/ZnO NW heterostructure arrays have improved photocatalytic activities compared with the bare ZnO nanowire array. We expect that the CdS NP/ZnO NW heterostructure arrays will offer promising applications as photocatalysts, photoelectrodes and also solar-energy conversion materials.

This work was supported by grant no. R01-2006-000-10230-0 (2006) from the Korea Science and Engineering Foundation, grant no. RTI04-01-04 from the Regional Technology Innovation Program of the Ministry of Commerce, Industry and Energy (MOCIE), and the Korean Research Foundation Grants funded by the Korean Government (MOEHRD) (KRF-2005-005-J13101).

Notes and references

1 M. R. Hoffmann, S. T. Martin, W. Choi and D. W. Bahnmann, *Chem. Rev.*, 1995, **95**, 69.
2 V. M. Aroutiounian, V. M. Arakelyan and G. E. Shahnazaryan, *Sol. Energy*, 2004, **78**, 581.
3 H. Fujii, M. Ohtaki, K. Eguchi and H. Arai, *J. Mol. Catal. A: Chem.*, 1998, **129**, 61; P. V. Kamat, *Chem. Rev.*, 1993, **93**, 267.
4 K. R. Gopidas, M. Bohorquez and P. V. Kamat, *J. Phys. Chem.*, 1990, **94**, 6435; J. E. Evans, K. W. Springer and J. Z. Zhang, *J. Phys. Chem.*, 1994, **101**, 6222.
5 F. Lu, W. Cai and Y. Zhang, *Adv. Funct. Mater.*, 2008, **18**, 1.
6 J. Yang, S. An, W. Park and G. Yi, *Adv. Mater.*, 2004, **16**, 1661; T. Kuo, C. Lin, C. Kuo and M. H. Huang, *Chem. Mater.*, 2007, **19**, 5143.
7 T. Sun, J. Qiu and C. Liang, *J. Phys. Chem. C*, 2008, **112**, 715.
8 Y. Tak and K. Yong, *J. Phys. Chem. B*, 2005, **109**, 19263; Y. Tak and K. Yong, *J. Phys. Chem. C*, 2008, **112**, 74.
9 R. Memming, *Electrochim. Acta*, 1980, **25**, 77; S. Hotchandani and P. V. Kamat, *J. Phys. Chem.*, 1992, **96**, 6834; J. Lee, Y. Sung, T. Kim and H. Choi, *Appl. Phys. Lett.*, 2007, **91**, 113104.
10 M. Xiao, L. Wang, Y. Wu, X. Huang and Z. Dang, *Nanotechnology*, 2008, **19**, 015706; J. Wang, Z. Liu, Q. Zheng, Z. He and R. Cai, *Nanotechnology*, 2006, **17**, 4561.
11 W. Shangguan and A. Yoshida, *J. Phys. Chem. B*, 2002, **106**, 12227; R. Jin, W. Gao, J. Chen, H. Zeng, F. Zhang, Z. Liu and N. Guan, *J. Photochem. Photobiol., A*, 2004, **162**, 585.